

## **Influence of coconut fiber incorporation on the mechanical behavior of adobe blocks**

N.A. da Silva<sup>1,2</sup>, D. Cecchin<sup>1,\*</sup>, C.A.A. Rocha<sup>1</sup>, R.D. Toledo Filho<sup>2</sup>, J. Pessin<sup>1</sup>, G. Rossi<sup>3</sup>, G. Bambi<sup>3</sup>, L. Conti<sup>3</sup> and P.F.P. Ferraz<sup>4</sup>

<sup>1</sup>Federal Fluminense University - UFF, Department of Agricultural and Environmental Engineering; Rua Passo da Pátria, 156, PO Box 21065-230, Niterói, Brazil

<sup>2</sup>Federal University of Rio de Janeiro - UFRJ, Civil Engineering Department, Rio de Janeiro, Brazil

<sup>3</sup>University of Firenze, Department of Agriculture, Food, Environment and Forestry (DAGRI), Via San Bonaventura 13, IT50145 Firenze, Italy

<sup>4</sup>UFPA - Federal University of Lavras, Department of Agricultural Engineering, Campus Universitário, PO Box 3037, Lavras, Minas Gerais, Brazil

\*Correspondence: [daianececchin@id.uff.br](mailto:daianececchin@id.uff.br)

Received: January 31<sup>st</sup>, 2024; Accepted: June 7<sup>th</sup>, 2024; Published: July 11<sup>th</sup>, 2024

**Abstract.** Adobe is an ancient construction technique, simple and low cost, still used in some parts of the world, mainly in rural areas. Normally, in these regions, a considerable amount of agricultural waste is generated that can be used for different purposes. An agricultural waste that has been increasingly studied in the construction sector is natural fibers. The addition of natural fibers in the soil matrix has been gaining prominence as it is a natural and easily accessible stabilizer. This work aimed to analyze and characterize adobe blocks reinforced with coconut fibers, with the addition of 1% and 2% compared to the reference block (without the addition of coconut fiber) through capillary absorption, fiber-soil adhesion, durability in the presence of water and mechanical, properties through of compression bending tests. The adobe blocks with the addition of fibers showed mechanical results above those required by the standard NBR 16814. The addition of fibers promoted higher capillary absorption results than the samples consisting only of soil and when exposed to drip erosion, no significant damage was observed in the adobe structure.

**Key words:** adobe, coconut fiber, rural buildings.

### **INTRODUCTION**

The construction with earth resurged significantly in 1970, where the global scenario was witnessing the oil crisis and the increasing environmental issues such as the rise in pollutant emissions related to high energy consumption and extraction of non-renewable raw materials (Santos & Lima Bessa, 2020). A technique used in the past in prehistoric dwellings reemerges as a low-cost, highly available, and environmentally friendly alternative (Cordeiro et al., 2020).

In Brazil, an important milestone occurred in 2020 regarding earthen construction, which was the publication of the standard NBR 16814 by the Brazilian Association of Technical Standards (ABNT, 2020a). This brought visibility and credibility to the adobe construction technique.

Adobe is the most commonly used technique due to its ease of fabrication (Jalali & Eires, 2008). Christoforou et al. (2016) conducted a cradle-to-gate Life Cycle Assessment (LCA) of adobe blocks under different scenarios. In the local production scenario with regionally sourced soil and reinforcement, the global warming potential (GWP) impact category was  $1.76 \times 10^{-3}$  kgCO<sub>2</sub>eq. The embodied energy value was 0.34 MJ/block, demonstrating that adobe has a significantly lower energy footprint than concrete blocks (12.5 MJ/block) and fired clay bricks (4.25 MJ/block).

When associated with rural constructions, it is an interesting alternative not only because of the ease of construction but also because it requires simple maintenance, low cost, and contributes to sustainable rural development in construction when compared to conventional building materials.

According to Faostat data, in 2019, the global production of coconut was 62.9 million tons, and Brazil was the fifth largest producer globally, accounting for 3.7% of the total produced, behind only Indonesia, the Philippines, India, and Sri Lanka (FAOSTAT, 2021). Coconut is frequently found in places with tropical climates, such as Brazil, and the residue from its processing, when not discarded properly, can create environmental problems (Lertwattanakul & Suntijitto, 2015). Natural fibers have been increasingly utilized in construction materials due to their characteristics and potential to enhance the mechanical properties of products (Ferreira et al., 2021). Among these fibers, acai fiber (Rocha et al., 2021), pineapple fibers (Azevedo et al., 2021), and coconut fibers (Ferreira et al., 2022) have been mentioned.

The characteristics of coconut residues include reduced cost, high lignin content, low density, abundant availability, while the fibers have high elongation at break, and low modulus of elasticity (Adeniyi et al., 2019). These characteristics of coconut residues make coconut fibers a promising choice as reinforcement for adobe blocks, as they can improve their mechanical properties. The objective of this study was to evaluate adobe blocks reinforced with the addition of coconut fiber for potential use in rural constructions. By investigating this combination, the study hopes to contribute to the development of more sustainable and accessible construction techniques, promoting both economic and environmental benefits.

## MATERIALS AND METHODS

### Soil

The soil used in the research was derived from excavation at a construction site in the state of Rio de Janeiro. Physical characterization tests (bulk density, moisture content, liquid limit, plastic limit, and plasticity index), granulometric analysis, and chemical composition analysis were conducted.

For the granulometric analysis, the soil was prepared according to the NBR 7181 (ABNT, 2016a) standard, which determines analysis by sieving and sedimentation (to distinguish the silt and clay fractions). In this study, the sedimentation test was replaced by laser diffraction analysis using the MasterSizer 2000 equipment, which provides precise

grain size measurements down to 0.0001 mm. It employs a light scattering technique where the angles of laser diffraction are measured and related to particle diameters.

The bulk density was determined according to NBR 6458 (ABNT, 2016b). Fifty grams of soil were separated, immersed in distilled water for 24 hours, and then transferred entirely to the dispersion cup and dispersed for 15 minutes. Subsequently, the sample was transferred to the pycnometer, where vacuum was applied to remove all air. After the test was completed, the set (pycnometer + soil + water) was weighed.

For determining the moisture content, the procedure followed the NBR 6457 (2016) standard. Three samples of 30 g each were taken in metallic capsules. The capsules along with the soil were weighed initially and then placed in an oven at 105 °C until a constant mass was achieved. Subsequently, the set was weighed again, the dry mass was recorded, and the moisture content was calculated according to Eq. (1).

$$w(\%) = \frac{Mu - Ms}{Ms} \times 100 \quad (1)$$

where  $w$  – Soil moisture content;  $Mu$  – Mass of the soil in its natural state;  $Ms$  – Mass of the soil when dry.

The plasticity index of the soil was determined by the decrease in the liquid limit, which is found through the test described in NBR 6459 (ABNT, 2016c), and the plastic limit test conducted according to NBR 7180 (ABNT, 2016d). The Liquid Limit (LL) is the transition from the liquid state to the plastic state, and the Plastic Limit (PL) is the transition from the plastic state to the semi-solid state. The Plasticity Index (PI) physically represents the amount of water needed to add to the soil to transition it from the plastic to the liquid state.

For the plastic limit test, 50 g of soil, a glass plate, and an oven were required. The soil used was the one passing through a 0.42 mm sieve. This soil was mixed with distilled water in a porcelain container until a homogeneous mixture was obtained. Then, 10 g of this sample was taken and formed into a small ball, which was rolled on the glass plate to form a cylinder with a diameter of 3 mm and a length of 100 mm. When the cylinder fragmented with these dimensions, the sample was transferred to a container, weighed, and placed in the oven to determine its moisture content. To determine the liquid limit, the Casagrande apparatus and 200 g of soil were required. After preparing the soil, a portion was transferred to the Casagrande apparatus. Once the apparatus was filled, a chisel was used to divide the material, and the apparatus was operated to perform the necessary blows until the lower edges of the groove joined. After this process, a portion of the soil was removed to determine the moisture content, and this test was repeated two more times to obtain mixtures covering the range of 15 to 35 blows. With the results obtained, a graph of the number of blows versus moisture content was plotted, and the liquid limit of the soil is the moisture content corresponding to 25 blows.

The chemical composition was determined through X-ray fluorescence (XRF) analysis using the Shimadzu model EDX-720.

### **Coconut fiber**

The coconut fibers used were purchased from the company Coco Verde, located in Duque de Caxias, Rio de Janeiro. The fibers were subjected to a crusher, with the aim of reducing their length and contributing to the adobe production process.

The coconut fibers underwent physical characterization (bulk density and moisture content) and Scanning Electron Microscopy (SEM) analysis. The moisture content of

the coconut fiber was determined according to the NBR 9939 standard (ABNT, 2011). Three samples of 30 g each were separated and distributed in metal trays, then placed in an oven at 105 °C until reaching a constant mass.

To determine the bulk density, the procedure followed the NBR NM 52 (ABNT, 2009) standard. Initially, the fibers were submerged in water for 24 hours and then exposed to air to superficially dry. They were then placed in bottles with water up to the 500 ml mark. The bottles were left to rest in a water bath at 21 °C for 1 hour. Afterward, the bottles were topped up with water, and the entire set was weighed to record the total mass. Finally, the samples were removed and placed in ovens to dry at 105 °C until a constant mass was achieved.

### Adobe

**Adobe Production.** Nine adobe blocks were produced (three for each treatment) and the production steps were as follows:

a. Production of wooden molds: The dimensions of the adobe mold were based on the criteria established by NBR 16814 (ABNT, 2020a), which are: 7×15×31 cm (height × width × length).

b. Preparation of the mixture: Three different mixtures were prepared, including a reference mixture with soil and water, and two others with the addition of 1% and 2% of fiber relative to the soil mass. The water-to-soil ratio was fixed at 0.35.

c. Molding and demolding: With the mixture ready, the mold was completely filled, the surface was leveled, and the adobe was demolded onto a flat surface.

d. Drying: The drying time was 20 days, ensuring uniform drying on all faces of the block.

**Analysis.** The adobe blocks underwent tests for: Mechanical characterization (uniaxial compression and flexural strength), absorption, density, durability, erosion test), and fiber-soil interface (pull-out test).

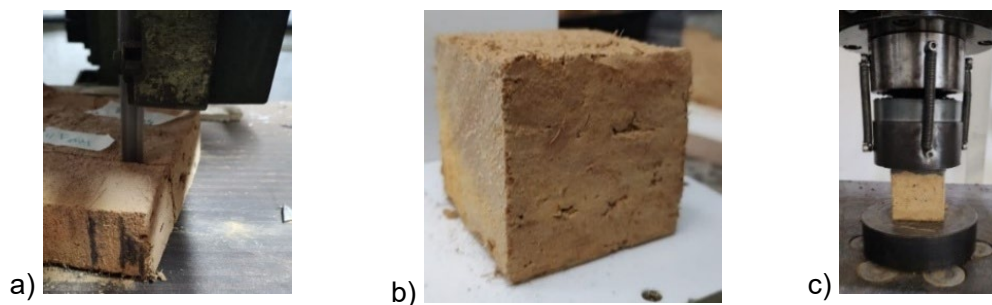


**Figure 1.** Uniaxial compression test: (a) sample cutting; (b) samples after cutting; and (c) uniaxial compression test of the adobe.

The uniaxial compression test was conducted according to NBR 16817 (ABNT, 2020b) standards using a Universal Testing Machine with a load capacity of 1,000 kN at a speed of 0.30 MPa min<sup>-1</sup>. Two cubic test specimens of 6 cm were cut from each adobe block using a band saw (Fig. 1, a and b). To regularize the faces, a capping layer of up to 3 mm thickness was applied using a mix of cement and fine sand in a ratio of 1:2 by mass. The setup of the tests is illustrated in Fig. 1, c.

The flexural test was conducted using a Shimadzu Universal Testing Machine with a loading capacity of 100 kN. The test speed used was 0.3 mm min<sup>-1</sup>. Prismatic specimens measuring (40×40×160 mm) were positioned for the three-point flexural test with a support span of 120 mm (Fig. 2).

For the calculation of flexural strength, Eq. (2) was used, according to the Araya-Letelier et al. (2019).

$$\tau_f = \frac{3PL}{2BH^2} \quad (2)$$

where  $P$  – maximum applied load;  $L$  – distance between supports;  $B$  – width of the sample;  $H$  – height of the sample.

The density of the blocks was determined according to BS EN 771:1 (2003). According to the standard, the specimens were placed in ovens at 110 °C for 48 hours until a constant mass was reached, and then weighed. The dimensions are collected, and the volume is calculated. Density is calculated using Eq. 3.

$$\rho = \frac{m}{V} \quad (3)$$

where  $\rho$  – density (kg m<sup>-3</sup>);  $m$  – mass (kg);  $V$  – volume (m<sup>3</sup>).

For the determination of water absorption by capillarity, the procedures were based on the NBR 9779 (ABNT, 2012) standard. The specimens were placed in an oven at 105 °C for 24 hours, and after this process, they were cooled to room temperature to determine their masses. Then, they were wrapped with plastic film, leaving a 5 mm strip without plastic, as it is the region that was in direct contact with water. The specimens were immersed in a 5 mm layer of water, arranged in a glass container. During the test, the mass of the specimens was recorded at 3, 6, 24, 48, and 72 hour intervals.

The drip erosion test was based on the NBR 17014 standart (ABNT, 2022). In this test, the block was placed on a surface with a 1:2 slope so that the center of gravity of the larger face is on the axis of water drip application. A container with 100 mL of water was positioned 400 mm above the block. Water dripped onto the block for approximately 30 minutes, and after this process, the depth of the hole was measured using a vernier caliper and ruler. Depending on the depth, the adobe mixture can be classified as erosive, highly erosive, or failure.

The analysis of the fiber-soil interface was conducted through the pullout test, where the fiber is pulled out of the soil, and force and displacement data are collected, performed as described by Mendonça (2018). To conduct this test, a machine called Tytron 250 was used, equipped with a 50 N load cell. The test speed was set at 0.4 mm min<sup>-1</sup>, and the samples consisted of a coconut fiber inserted into a PVC tube filled with soil, with an immersion length of 10 mm. For the calculation of the maximum tension ( $\tau_{m\acute{a}x}$ ), it was compute using Eq. (4)

$$\tau_{m\acute{a}x} = \frac{P_{m\acute{a}x}}{lfPe} \quad (4)$$

where  $P_{m\acute{a}x}$  – maximum load during pullout;  $lf$  – fiber embedment length;  $Pe$  – fiber perimeter.



**Figure 2.** Three-point flexural test.

To obtain the perimeter of the fiber, images from the SEM (Scanning Electron Microscope) and the Image J software were used.

## RESULTS AND DISCUSSION

### Soil

The grain size distribution curve of the soil is presented in Fig. 3, where the grain diameters and the percentages retained and passed through the soil are observed, according to the distribution of sieves described in NBR 7181 (ABNT, 2016).

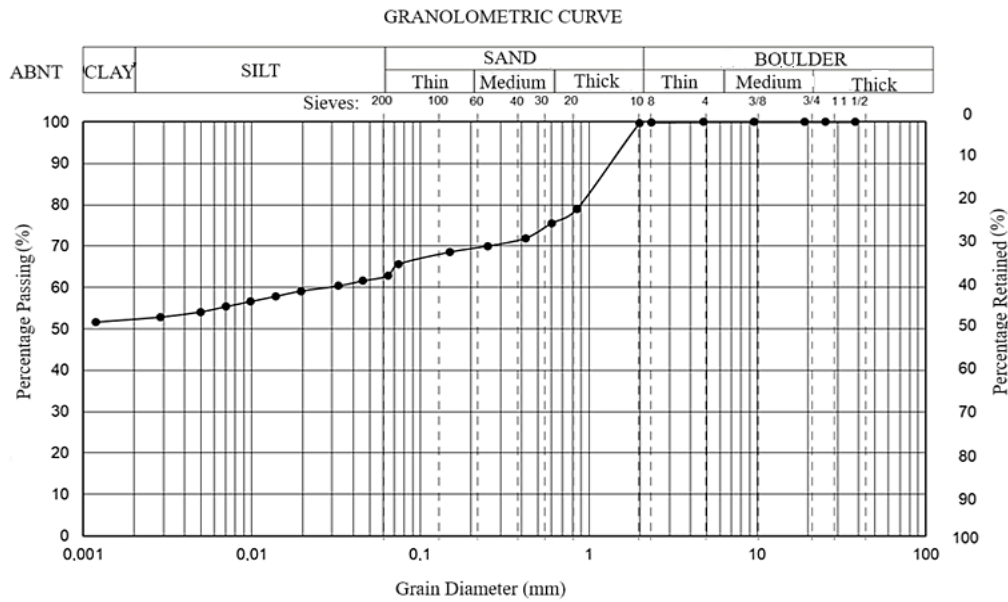


**Figure 3.** Granulometric distribution curve of the soil.

The grain size composition of the soil (Table 1) showed a higher concentration of clay (52%), followed by sand (37%), and finally silt (10%). According to NBR 16184 ABNT, 2020), the grain size composition should preferably meet (the following parameters: sand (between 45% and 65%); silt (up to 30%); and clay (between 25% and 35%).

Analyzing the grain size distribution of the soil selected for this study, the clay and sand contents do not meet the parameters specified by the standard. In this case, the standard suggests conducting physical and mechanical behavior tests on the produced adobes to determine if they meet performance specifications.

The results of the soil's physical properties can be observed in Table 2.

**Table 1.** Granulometric composition of the soil

Gravel	Coarse Sand	Medium Sand	Fine Sand	Silt	Clay
1%	24%	6%	7%	10%	52%

**Table 2.** Soil physical properties and coefficient of variation (in parentheses)

Bulk density (BD)	Plastic limit (PL)	Liquid limit (LL)	Plasticity index (PI)	Moisture Content (MC)
2.37 g cm <sup>-3</sup> (2.19)	31.65% (4.50)	56.25% (6.12)	24.75%	3.11% (0.80)

The average soil moisture content at the time of the test was 3.11%, and the bulk density was  $2.37 \text{ g cm}^{-3}$ . When analyzing the consistency limits, it is important to note that this property is related to the physical state in which the soil is found in the presence of moisture and is divided into four groups: liquid (soil with fluid appearance), plastic (moldable soil), semi-solid (soil that shrinks when drying), and solid (soil that no longer undergoes volumetric variation) (Silva, 2022). According to Burmister (1949), a soil with a PI between 20–40, which is the case of the soil in this study (24.75%), is considered to have high plasticity, a characteristic of more clayey soils. Table 3 presents the chemical composition of the soil in the form of oxides, and it is noticeable that the highest contents are silica ( $\text{SiO}_2$ ), alumina ( $\text{Al}_2\text{O}_3$ ), and hematite ( $\text{Fe}_2\text{O}_3$ ). According to Brian & Carleton (1982), these chemical elements, after oxygen, are the most abundant in the Earth's crust, and these contents may vary in percentages depending on the location.

**Table 3.** Chemical composition of the soil

Element	Content (%)
$\text{SiO}_2$	41.13
$\text{Al}_2\text{O}_3$	38.43
$\text{Fe}_2\text{O}_3$	15.78
$\text{SO}_3$	1.66
$\text{TiO}_2$	1.55
BaO	0.66
$\text{K}_2\text{O}$	0.26
others	0.53

### Coconut fiber

The bulk density and moisture content of coconut fibers yielded the following results and coefficients of variation, respectively:  $1.06 \text{ g cm}^{-3}$  (8.4) and 8.77 (4.1). Vegetable fibers in general do not have a defined cross-section, and their dimensions can vary along the length (Ribeiro, 2021). Fig. 4, a shows an image of the cross-section of coconut fiber, which appears to have an approximately circular shape.

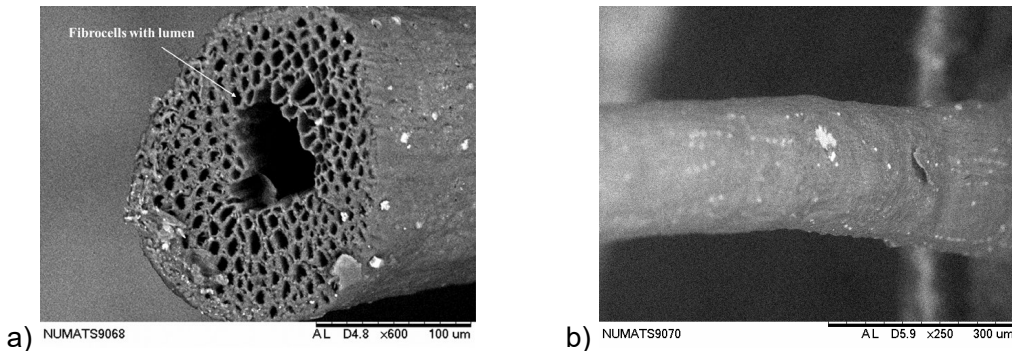


**Figure 4.** Scanning Electron Microscopy (SEM) images of coconut fibers: a) cross-section and b) outer surface.

Coconut fibers have a significant number of fibrocells, and their cell walls are thinner compared to other vegetable fibers such as sisal, jute, and curauá (Pereira, 2012). In Fig. 4, b, the outer surface of the fiber can be analyzed, showing a slight roughness that, according to Nunes et al. (2022), may be due to its vegetal origin and the extraction processes, which can result in the presence of impurities, fats, and organic residues adhered.

### Adobe

The values of bulk density of the adobe blocks (reference (without fiber addition), 1% fiber addition, and 2% fiber addition) and their respective coefficients of variation were:  $1,790 \text{ kg m}^{-3}$  (4.1),  $1,714.77 \text{ kg m}^{-3}$  (3.6) and  $1,675 \text{ kg m}^{-3}$  (2.4). Since coconut fibers are very light (density  $1.06 \text{ g cm}^{-3}$ ), when incorporated into the soil matrix, there is a reduction in densities compared to the reference mixture. This reduction ranges from 4.20% for the mixture with 1% of fibers to 6.40% for the mixture with 2% of fibers.

In the adobe blocks reinforced with fibers, an increase in water absorption by capillarity is observed (Fig. 5). This increase is attributed to the water absorbed by the cellulose of the fibers and the voids created by the fibers in the blocks, allowing more water to be absorbed. During the mixing process, the fibers absorb water and expand, and after the drying process, the fibers retract, creating these voids (Ghavami et al., 1999; Danso et al., 2015).

Upon analyzing the results from the drip erosion analysis, it was noted that there were no significant changes on the surface of the blocks. In fact, the 17014 standard (ABNT, 2022) recommends dripping 100 mL of water onto the block's surface for 20 to 60 minutes. In this study, double the amount of water was tested, and consequently, the time also doubled, to simulate a more severe scenario. However, no significant impact was observed.

According to Danso et al. (2015), when using water jets with higher pressures, the durability of the blocks is more affected. The authors concluded that fiber-reinforced blocks protect soil particles from being carried away, thus reducing the effects of erosion.

For the analysis of fiber-soil adhesion, the coconut fiber was inserted into the matrix and subjected to a tensile force. As the fiber displaced, a force-displacement curve of the fiber was obtained (Fig. 6). According to Naaman et al. (1991), the adhesion between fiber and matrix is a result

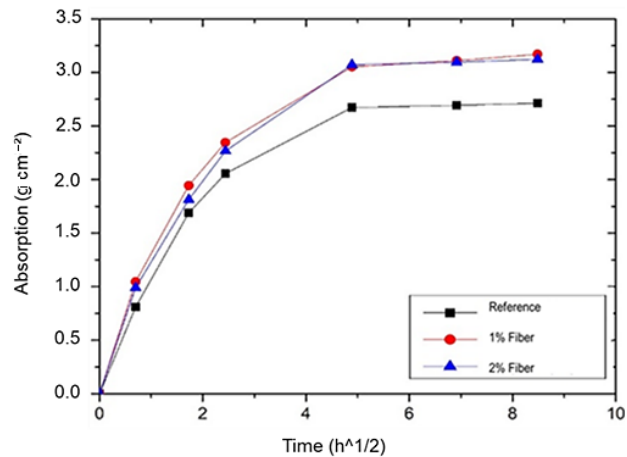


**Figure 5.** Capillary absorption curves of the adobe blocks.

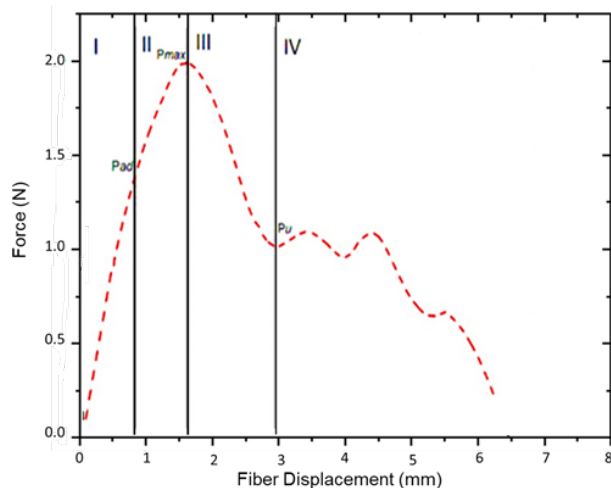


**Figure 6.** Typical force-displacement curve of the fiber from the pull-out test.



of the combined action of many elements, including physical-chemical adhesion between the fiber and the matrix, anchorage, and friction.

According to Ribeiro (2021), this behavior can be divided into four phases: Phase I: In this initial phase, the behavior is linear until the point where the superficial shear stress results in the breakage of the chemical adhesion between the fiber and the matrix, at which point the  $P_{ad}$  (adhesion load) is reached. Analyzing the curve, it is noted that in the case of coconut fiber with the soil matrix, this breakage of chemical adhesion occurred at 1.2 N. Phase II: The displacement is no longer linear, and partial decohesion of the fiber-matrix interface occurs until the pull-out force reaches the maximum value,  $P_{max}$  (2N). With this load, it was possible to calculate the adhesive stress ( $\tau_{max}$ ), which was 0.28 MPa, as shown in Table 4. Phase III: In the post-peak phase, the fiber was gradually pulled out of the matrix, reducing the force. The fissure of the fiber-matrix interface, which began in phase II, propagates throughout the fiber's length, characterized by the point  $P_u$  (0.88 N). Phase IV: It is characterized by the total pull-out of the fiber along its embedding length.

**Table 4.** Average results and coefficient of variation of the coconut fiber pull-out test

Perimeter ( $\mu\text{m}$ )	$P_{ad}$ (kN)	$P_{max}$ (kN)	$P_u$ (kN)	$\tau_{max}$ (MPa)
1,027.92 (9.4)	1.20 (8.7)	2.00 (5.6)	0.88 (7.8)	0.28 (3.2)

$P_{ad}$ : adhesion load;  $P_{max}$ : peak load;  $P_u$ : fiber debonding force;  $\tau_{max}$ : bond stress.

The uniaxial compression strength was analyzed according to NBR 16814 (ABNT, 2020a), where the individual compression strength of adobe should be  $\geq 1.5$  MPa. All mixtures produced and tested in this study were above 1.5 MPa (Table 5), hence they can be used in constructions. It is noticeable that as the fiber content increases, the compression strength reduces. This phenomenon is related to the porosity of the material, which can cause additional microcracks due to fiber detachment and the formation of cracks at the fiber-matrix interface (Li, 1992; Ribeiro, 2021).

**Table 5.** Average results and coefficient of variation of the uniaxial compression test

Mixtures	$f_{ca}$ (MPa)	Coefficient of variation (%)
Reference (0% fiber)	2.19	8.37
1% fiber	2.05	6.50
2% fiber	1.95	9.50

Abdulla et al. (2020) investigated the mechanical properties of straw fiber-reinforced adobe and obtained a compressive strength of 1.45 MPa after 28 days of curing. Rodríguez-Mariscal & Solís (2020) evaluated the mechanical properties of unreinforced adobe blocks in compression and found a value of 1.13 MPa. Pinto et al. (2021) subjected unreinforced adobe blocks to compression and found a value of 1.97 MPa; when reinforced with sisal, the value significantly increased to 3.28 MPa. Comparing the values found in this study with those in the literature, it is evident that the results are within the observed ranges.

Regarding the behavior of adobes during rupture, it is important to note that this behavior begins with the formation of microcracks, and when fibers are added, there is a delay in the propagation of cracks, preventing catastrophic failure (Ribeiro, 2021). Fig. 7, b and 7, c represent this type of behavior, while Fig. 7, a shows that the reference formed a continuous crack map, leading to abrupt rupture shortly thereafter.

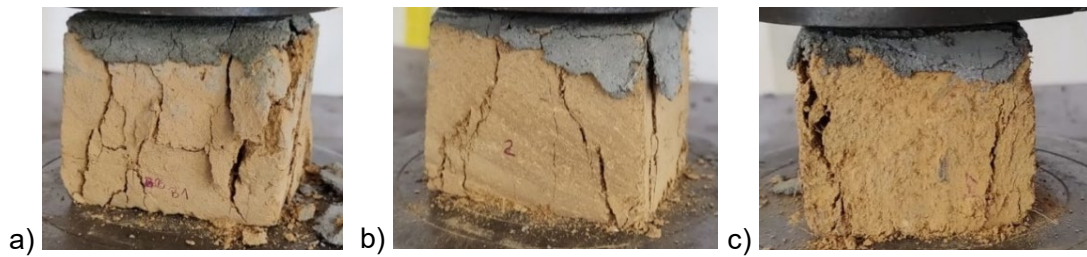


**Figure 7.** Samples broken after uniaxial compression test: a) reference (0% fiber); b) 1% fiber; and c) 2% fiber.

In regards to the three-point bending test, only the reference adobe blocks and those with 2% fiber were tested, as it has the highest volumetric fraction of fibers. The values obtained for flexural strengths (Fig. 8) for the reference adobe block were 0.61 MPa (6.8), and for the samples with 2% fiber, the strength was approximately 0.56 MPa (9.4).

The load-displacement curve of the reference sample initially exhibits a linear behavior, and when the first crack appears (peak), there is an abrupt reduction in load, classifying this behavior as brittle. The characteristic crack opening of these samples can be observed in Fig. 9. The curve representing the samples with 2% fiber initially shows a linear segment until the first crack, and as micro-cracking begins, the randomly arranged fibers limit this propagation, improving resistance and ductility. The rupture process is characterized by the pulling out of fibers until the opening of a single crack.

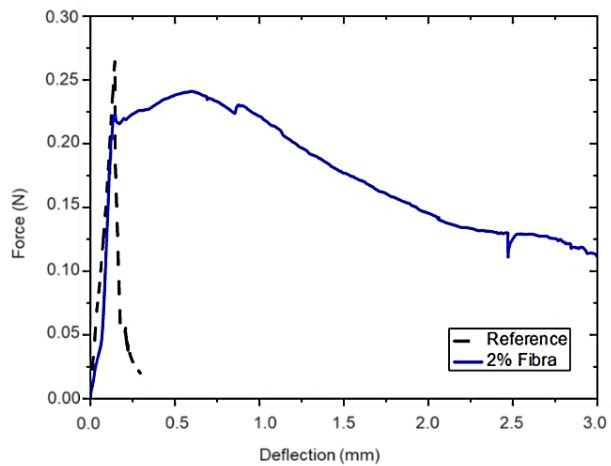


**Figure 8.** Load-displacement behavior of the adobe blocks.



**Figure 9.** Adobe samples after the bending test:(a) Reference and (b) 2% fiber.

## CONCLUSIONS

With the incorporation of fibers, there was a reduction in the apparent densities of the adobe blocks.

When inserted into the adobe production process, the fibers absorb a certain amount of water from the mixture, which leads to an expansion process of their structure. As the block drying process occurs over time, these fibers undergo a retraction process, and the fiber-matrix interface experiences micro-cracks that end up providing pathways for a greater amount of water to penetrate, resulting in higher capillary absorption.

The evaluated adobe blocks did not show any significant damage related to water erosion when exposed to water dripping.

All blocks surpassed 1.5 MPa when subjected to compression loads, confirming the potential application of adobe. It was observed that the fibers provided mechanical gains regarding both the rupture and stabilization of the blocks, not only in compression but also in flexion.

Applying coconut fibers in earth constructions, specifically adobe, is a safe, low-cost possibility that requires low technology and contributes to the environment.

For future research, it is suggested to test the durability of adobe blocks under different climatic conditions by exposing them to prolonged cycles of rain, sun, wind, and temperature variations. Additionally, it is proposed to explore other natural fibers such as jute, sisal, and bamboo, with the aim of identifying alternatives that can further improve the strength and sustainability of these construction materials.

ACKNOWLEDGEMENTS. To the Ministério da Agricultura, Pecuária e Abastecimento (MAPA) for the scholarship granted to the first author during the Postgraduate Course - Residency in Agricultural Practices and Technical Assistance and Rural Extension (ATER).

## REFERENCES

- Abdulla, K.F., Cunningham, L.S. & Gillie, M. 2020. Experimental study on the mechanical properties of straw fiber-reinforced adobe masonry. *Journal of Materials in Civil Engineering* **32**(11), 04020322. doi\_ 10.1061/(asce)mt.1943-5533.0003410
- ABNT - Associação Brasileira de Normas Técnicas. 2016a. *Soil-Particle Size Analysis*, NBR 7181, ABNT: Rio de Janeiro, Brazil, 2016, 12 pp. (in Portuguese).
- ABNT - Associação Brasileira de Normas Técnicas. 2016d. *Soil-Determination of Plastic Limit*, NBR 7180; ABNT: Rio de Janeiro, Brazil, 2016; 3 pp. (in Portuguese)
- ABNT - Associação Brasileira de Normas Técnicas. 2020a. *Adobe - Requirements and Testing Methods*, NBR 16814 Rio de Janeiro, Brazil (in Portuguese).
- ABNT - Associação Brasileira de Normas. 2009. *Fine Aggregate - Determination of Specific Gravity and Apparent Specific Gravity*, NBR NM 52, Rio de Janeiro, Brazil, 6 pp. (in Portuguese)
- ABNT - Associação Brasileira de Normas. 2011. *Coarse Aggregate - Determination of Total Moisture Content - Test Method*, NBR 9939, ABNT: Rio de Janeiro, Brazil, 3 pp. (in Portuguese).
- ABNT - Associação Brasileira de Normas. 2012. *Hardened mortar and concrete - Determination of water absorption by capillarity*, NBR 9779, ABNT: Rio de Janeiro, Brazil, 3 pp. (in Portuguese).
- ABNT - Associação Brasileira de Normas. 2016c. *Soil-Determination of Liquid Limit*, NBR 6459, ABNT: Rio de Janeiro, Brazil, 2016, 5 pp. (in Portuguese).

- ABNT - Associação Brasileira de Normas. 2020b. *Non-destructive testing - Conventional radiography - Procedure qualification* NBR 16817, ABNT: Rio de Janeiro, Brazil, 4 pp. (in Portuguese).
- ABNT - Associação Brasileira de Normas. 2022. *Rammed earth construction - Requirements, procedures, and control*, NBR 17014, Rio de Janeiro, Brazil, 34 pp. (in Portuguese).
- Adeniyi, A.G., Onifade, D.V., Ighalo, J.O. & Adeoye, A.S. 2019. A review of coir fiber reinforced polymer composites. *Composites Part B: Engineering* **176**, 107305. doi: 10.1016/j.compositesb.2019.107305
- Araya-Letelier, G., Concha-Riedel, J., Antico, F.C. & Sandoval, C. 2019. Experimental mechanical-damage assessment of earthen mixes reinforced with micro polypropylene fibers. *Construction and Building Materials* **198**, 762–776. doi: 10.1016/j.conbuildmat.2018.11.261
- Azevedo, A.R.G., Rocha, H.A., Marvila, M.T., Cecchin, D., Xavier, G.C., Silva, R.C., Ferraz, P.F.P., Conti, L. & Rossi, G. 2021. Application of pineapple fiber in the development of sustainable mortars. *Agronomy Research* **19**(3), 1387–1395, doi: 10.15159/AR.21.140
- Brasileira de Normas Técnicas. 2016b. *Soil Sample—Preparation for Compaction Tests and Characterization Tests*, NBR 6457, ABNT: Rio de Janeiro, Brazil, 8 pp. (in Portuguese).
- Brian, M. & Carleton, B.M. 1982. *Principles of geochemistry*. 4.ed. New York, John Wiley, 344 pp.
- BRITISH STANDARDS INSTITUTION. 2003. *BS EN 771-1: Specification for masonry units—Part 1: Clay masonry units*.
- Burmister, D.M. 1949. Principles and techniques of soil identification. In: *Proceedings of the Highway Research Board. National Research Council*. Washigton, DC **29**, 402–434.
- Christoforou, E., Kylili, A., Fokaides, P.A. & Ioannou, I. 2016. Cradle-to-Site Life Cycle Assessment (LCA) of adobe bricks. *Journal of Cleaner Production* **112**, 443–452 (in Portuguese).
- Cordeiro, C.C.M., Brandão, D.Q., Durante, L.C., Callejas, I.J.A. & Campos, C.A.B. 2020. Thermophysical characterization of lateritic soil for manufacturing rammed earth walls. *Matéria (Rio de Janeiro)* **25**(1) e-12564. doi: 10.1590/S1517-707620200001.0889
- Danso, H., Martinson, B., Ali, M. & Williams, J. 2015. Effect of fibre aspect ratio on mechanical properties of soil building blocks. *Constr. Build. Mater.* **83**, 314–319. <https://doi.org/10.1016/j.conbuildmat.2015.03.039>
- FAOSTAT (Food and Agriculture Organization of The United Nations). 2021. *Crops and livestock products*. Available on: <https://www.fao.org/faostat/en/#data/>. Accessed in: 18 jan 2024.
- Ferreira, G.M.G., Cecchin, D., De Azevedo, A.R.G., Valadão, I.C.R.P., Costa, K.A., Silva, T.R., Ferreira, F., Amaral, P.I.S., Huther, C.M. & Sousa, F.A. 2021. Bibliometric analysis on the use of natural fibers in construction materials. *Agronomy Research* **19**, 1–12. doi: 10.15159/AR.21.131
- Ferreira, G.M.G., Cecchin, D., Valadão, I.C.R.P., da Silva, T.R., do Carmo, D.d.F., Moll Hüther, C., Ferreira, F. & de Azevedo, A.R.G. 2022. Evaluation of the Technological Properties of Soil–Cement Bricks with Incorporation of Coconut Fiber Powder. *Eng.* **3**(3), 311–324. <https://doi.org/10.3390/eng3030023>
- Ghavami, K., Toledo Filho, R.D. & Barbosa, N.P. 1999. Behaviour of composite soil reinforced with natural fibres. *Cement and Concrete Composites* **21**(1), 39–48. doi: 10.1016/S0958-9465(98)00033-X
- Jalali, S. & Eires, R. 2008. *Scientific Innovations in Earthen Construction*. In: *Internacional Conference-Angola: Teaching, Research and Development* (EIDAO 080), 7. (in Portuguese).
- Lertwattanaruk, P. & Suntijitto, A. 2015. Properties of natural fiber cement materials containing coconut coir and oil palm fibers for residential building applications. *Constr. Build. Mater.* **94**, 664–669. doi: 10.1016/j.conbuildmat.2015.07.154

- Li, V.C.A. 1992. Simplified micromechanical model of compressive strength of fiber-reinforced cementitious composites. *Cement and Concrete Composites* **14**(2), 131–141. doi: 10.1016/0958-9465(92)90006-H
- Mendonça, Y.G.S. 2018. *Micromechanical Dosage of Cementitious Composites Reinforced With Jute Fibers*. Master's Thesis, Federal University of Rio de Janeiro, Rio de Janeiro, Brazil, 120 pp. (in Portuguese).
- Naaman, A.E., Adce, M., Namur, G.C., Alwan, J.M. & Najm, H. 1991. Fiber pullout and bond slip. I: Analytical study. *Journal of structural engineering* **11**(9), 2769–2790.
- Nunes, J.V.S., da Silva, E.X.B., Miranda, M.H.P., Rios, A.S. & de Deus, E.P. 2022. Mechanical and Morphological Characterization of Surface-Treated Coconut Fibers for Use as Reinforcement in Polymers. *Matéria* **27**(2). doi: 10.1590/1517-7076-RMAT-2022-0046 (in Portuguese).
- Pereira, T.V.C., Fidelis, M.E.A., Gomes, O.F.M., Silva, F.A. & Toledo Filho, R.D. 2012. Investigation of Morphological Influence via Image Analysis on the Tensile Strength of Natural Fibers. In: *Congresso Anual da ABM, ABM WEEK-67*, Rio de Janeiro, Brasil, pp. 31–03. (in Portuguese).
- Pinto, B.R. 2021. *Thermal and mechanical performance of alkaline activated adobe masonry reinforced with sisal fiber*. Master's Thesis, Federal University of Paraíba, Paraíba, Brazil 146 pp. (in Portuguese).
- Pinto, B.R. 2021. *Thermal and mechanical performance of alkaline activated adobe masonry reinforced with sisal fiber*. Master's Thesis, Federal University of Paraíba, Paraíba, Brazil 146 pp. (in Portuguese).
- Rocha, H.A., Azevedo, A.R.G., Marvila, M.T., Cecchin, D., Xavier, G.C., Silva, R.C., Ferraz, P.F.P., Conti, L. & Rossi, G. 2021. Influence of different methods of treating natural açai fibre for mortar in rural construction *Agronomy Research* **19**(S1), 910–921. doi: 10.15159/AR.21.062
- Rodríguez-Mariscal, J.D. & Solís, M. 2020. Towards a methodology for the experimental characterization of the compressive behavior of adobe masonry. *Informes de la Construcción* **72**(557). doi: 10.3989/ic.67456 (in Spanish).
- Santos, D.P. & Lima Bessa, S.A. 2020. The Use of Adobe in Brazil: A Literature Review. *MIX Sustentável* **6**(1), 53–66 (in Portuguese).
- Silva, R.W.G.da. 2022. *Correlations for Preliminary Identification of Optimum Moisture Content of Brazilian Soils*. Trabalho de Conclusão de Curso. Universidade Federal do Rio Grande do Norte, 18 pp. (in Portuguese).